J. Physiol. (1983), **336**, *pp.* 527–543
With 7 *text-figures*
Printed in Great Britain

EXPERIMENTAL ANALYSIS OF ALTERNATIVE MODELS OF CHARGE MOVEMENT IN FROG SKELETAL MUSCLE

By C. L.-H. HUANG
From the Physiological Laboratory, University of Cambridge, Downing Street, Cambridge

(*Received 27 April 1982*)

SUMMARY

1. A series of pulse procedures was used to distinguish experimentally between a 'capacitative' (Schneider & Chandler, 1973) and a 'resistive' (Matthias, Levis & Eisenberg, 1980) model of 'charge movements' in skeletal muscle.

2. A general condition describing the conservation of charge in a non-linear capacitor that was used as the basis for the experiments is derived in the Appendix.

3. It was shown that earlier criteria concerning equality of 'on' and 'off' charge in response to large steps are insufficient to exclude resistive models.

4. However, the capacitative, but not the resistive model successfully explained results bearing on charge conservation assessed through pulse procedures involving: (i) small, 10 mV voltage steps from a series of prepulse voltages, (ii) voltage steps to a fixed potential from a series of hyperpolarized voltages, (iii) pulse sequences incorporating a 'staircase' of voltage steps.

5. It is concluded that the earlier use of 'on' and 'off' equality in response to large voltage steps is insufficient to exclude a resistive basis for the non-linear transient. However pulse procedures explicitly designed to distinguish the two models give results consistent with a capacitative model for the non-linear charge and at variance with a resistive one.

INTRODUCTION

The non-linear transients measured as 'charge movements' in response to applied voltage-clamp steps in skeletal muscle have usually been assumed to result from movement of voltage-dependent capacitative charge within a membrane rather than from ionic currents. Thus they persist in bathing solutions that would minimize ionic currents; furthermore non-linear charge (as computed by integrating the current transient $I(t)-I(\infty)$ to large voltage steps of sufficient duration to allow their full relaxation) was equal for the 'on' and 'off' parts of the imposed potential change (Schneider & Chandler, 1973). Similar arguments have been applied to related phenomena in nerve (e.g. Armstrong & Bezanilla, 1973). Furthermore, subsequent work on the charge movement in muscle (Chandler, Rakowski & Schneider, 1976) went on to consider a wide variety of alternative equivalent circuits in detail, and concluded that mechanisms other than those invoking non-linear capacitance were unlikely to explain the observation made of the non-linear charge, in particular the preservation of equal 'on' and 'off' charge to large voltage steps. However, more recently, Matthias, Levis & Eisenberg (1980, 1981) considered a different class of models of varying complexity, based on an equivalent circuit including a non-linear time- and voltage-dependent resistor R_x in series with a parallel resistance–capacitance (R–C) element in which the capacitor, C, was voltage-independent. They showed that selecting the appropriate time and voltage dependences in R_x would give the required 'on' and 'off' equality in the non-linear transient in response to large equal and opposite voltage steps of long duration. This result would seem to suggest that this usual test of 'on' and 'off' equality in the integral Q of the transient part of $I(t)$ is insufficient to establish its physical mechanism, and that further procedures would be necessary to resolve the two major possibilities (Gilly, 1981): (a) Q is capacitative as originally suggested by Schneider & Chandler (1973), with possibly some component relating to contractile activation (Huang, 1981*a*, 1982; Horowicz & Schneider, 1981) or (b) Q is the result of a time-dependent ionic current through access pathway R_x into sarcoplasmic reticulum (Matthias *et al.* 1980); this process may relate to contractile activation of muscle through the change which alterations in R_x would produce in the membrane potential of the terminal cisternae.

This paper uses a generalized condition of conservation of charge in a capacitor as the basis for pulse procedures used to compare the predictions of hypotheses (a) and (b) with experimental results. It derives the independence of the displaced capacitative charge $\int d\mathbf{Q}\, d\mathbf{r}$ of the path $\mathbf{r}(t)$ between given initial and final steady conditions in the voltage–temperature (V–T) plane. This condition is independent of the number of charge components involved or of any non-linearities present in the kinetics of the response of the system to imposed voltage change. The formalism employed also predicts the remaining major experimental observations concerning the charge movement. Thus voltage dependence, and saturation at large absolute values of applied potential, in addition to the generalized conservation of charge, follow analytically from the same equation. The capacitative model is thus the simplest available description of the observed steady-state phenomena, and is also readily testable using this preservation of charge. Nevertheless, the structural complexity of muscle continues to make the alternative resistive model a physical possibility. One possible insight into this model, which led to the approach used here in testing the alternatives, considers an over-simplified circuit consisting of resistor R_1 in series with elements $R_2\, C_2$ in parallel. For such a circuit, the integral of the transient non-linear response to an applied voltage step from V_0 to V can be written as a superposition integral:

$$\int_{V_0}^{V} dQ = \int_{V_0}^{V} \left(\frac{R_2}{R_1+R_2}\right)^2 C_2 \,.\, dV.$$

The resistive model asserts that $\int dQ$ is voltage-dependent through a non-linearity in R_1 rather than in the capacitative element, C_2, of the circuit. However, at the end of the step, the 'off' charge equalling the 'on' charge requires R_1 also to be time-dependent, $R_1(V, t)$, and to possess time constants whose voltage dependence ensures the condition $R_1(V_0, t) \simeq R_1(V, \infty)$ until the 'off' transient, $I(t')$, has almost fully relaxed. Introducing these non-linearities mean that $\int dQ$ has to be evaluated numerically. Furthermore, the smooth voltage dependences employed in the model to describe the coupled first-order processes defining R_1 (or g_x) as a function of time require the imposed voltage to be explicitly specified as a function of time, $V(t)$. This is in addition to the values of the initial and final steady state which is all that is required for the capacitative model. Thus the resistive model does not possess an explicit analytic condition defining charge as a function of steady-state voltage. It should therefore be possible to find driving voltages $V(t)$ of different form in which the rather limited conservation of charge condition, produced by the particular parameters employed for this model, breaks down. This is provided that the durations of the pulse procedures employed are short relative to the time course of charge immobilization through prolonged depolarization (Adrian & Almers, 1976). As all the voltage steps employed only had durations of the order of milliseconds, such charge inactivation was not observed in the present experiments. In contrast, under such conditions, charge remains a unique function of any pair of initial and final voltages through all paths under a capacitative model. This paper therefore uses voltage steps to consider these conditions, and compares the experimental results with the predictions from a capacitative, and from a resistive model.

METHODS

Experimental

The basic experimental layout has been described in greater detail elsewhere (Adrian & Rakowski, 1978) so only a brief account is given.

A three micro-electrode voltage clamp was imposed at the pelvic end of frog sartorius muscle fibres. The micro-electrodes were inserted 500 μm (clamp electrode, voltage, V_1), 1000 μm (V_2 electrode) and 1250 μm (current injection electrode, I_0) from the fibre end respectively. Transient currents, i_m (transient) moved by potential steps were examined. These were obtained using pulse procedures detailed in the Results. The currents were expressed as unit surface membrane area:

$$i_m(t) = \frac{d}{6l^2R_i}[V_2(t) - V_1(t)].$$

The areas under the transient part of the current, or charge moved, were computed by applying Simpson's Rule to the $i_m(t)$ arrays; leak admittances, given by $V_1(t)$ scaled by $i(\infty)/V_1(\infty)$, having been corrected for. The cable constants λ, r_i and r_m were calculated from the steady values of the voltages V_1 and V_2 and injected current I_0 at the end of a 10 mV step from the holding potential of -90 mV. Calculating fibre diameter, d, and specific membrane constants, employed a value of sarcoplasmic resistivity R_i of 391 Ωcm in hypertonic solution at 2 °C, and a Q_{10} of 1·37 (Hodgkin & Nakajima, 1972). Arrays representing $V_1(t)$, $V_2(t) - V_1(t)$ and $I_0(t)$ were obtained by analog-to-digital conversion, and sampled by an on-line PDP 11/10E computer (Digital Equipment Corporation, Maynard, MA, U.S.A.) at a sampling interval of 200 μsec/point. Signal averaging of up to 5–10 sweeps per average was employed, and every 2–3 averages at test potentials was followed by sweeps at -90 mV; cable analysis of such successive control sweeps checked the condition and stability of the fibre. Experiments were done at 3–6 °C in the following bathing solution: Rb_2SO_4, 5 mM; tetraethylammonium $(TEA)_2SO_4$, 80 mM: (TEA)Cl, 15 mM; $CaSO_4$, 8 mM; tetrodotoxin 2×10^{-7} M; Tris buffer, 3 mM; sucrose, 350 mM. All fibres were studied within 1–$1\frac{1}{2}$ hr of the bathing solution being substituted for the isotonic Ringer in which they were dissected.

Solution of differential equations

The results obtained were compared with solutions of the equations of the resistive model in its basic form, which was designed to produce charge conservation but not saturation. This is the model described fully in the paper (Appendix) of Matthias *et al.* (1980). The parameters used and their values and symbols are described in the Tables in their paper. Results of computed non-linear charge are normalized to the linear fibre capacitance in both experimental and theoretical results, as obtained by the 10 mV voltage step at the control and reference voltage. The numerical approach parallels that given in Matthias *et al.* (1980), and so is given in outline only, except where further optimizations are introduced and justified as follows:

(i) the driving function, $V_w(t)$ was computed as an array in increments equal to the stepsize Δt employed. The voltage step $H(t) . \Delta V_w$ was computed using the form $H(t) = \lim_{\tau \to 0} (1 - e^{-t/\tau})$ with τ successively decreased until computed solutions stayed constant.

(ii) Probability functions p_x, p_{1x}, given by the coupled first-order differential equations of the form

$$\frac{dp_x}{dt} = -a_x(V_w)(p_x - p_{1x}), \frac{dp_{1x}}{dt} = -a_x(V_w)(p_{1x} - N_x(V_w)),$$

were computed using a fourth-order Runge–Kutta method with successively decreased step size until no change in numerical solution resulted. Use of a fourth-order method rather than the first-order one originally used enhanced optimization with respect to step size.

(iii) The non-linear, differential, transcendental equation for the circuit,

$$F \equiv (\bar{g}_x \xi_x(V_x)\, p_x(t, V_w) + g_{x0})\,(V_x - E_x) - C_{TC}\frac{dV_w}{dt} + C_{TC}\frac{dV_x}{dt} - g_{TC}\, V_w + g_{TC}\, V_x = 0,$$

was solved in dV_w/dt iteratively for each time, t, by using a value of V_w determined by the previous value at $t - \Delta t$, and the iterated dV_w/dt, $V_w \simeq V_w(t - \Delta t) + \Delta t . dV_w/dt$. The solution to F was obtained using an algorithm directed at finding the real zero of any given function employing a choice of bisection, inverse quadratic, or secant interpolation depending upon the optimization required to achieve the maximum convergence of iterated solutions to give the function zero. The result was to a tolerance set equal to that of the machine epsilon on single-precision floating-point arithmetic (Brent, 1973). The advantage of this particular approach over the classical forward difference appoach is that solutions of $F = 0$ are determined for any time without their numerically lagging the driving function.

(iv) The initial values used in the above solutions were the steady-state ones, corresponding to the condition where derivatives of voltage are zero, given by the equation

$$(\bar{g}_x \xi_x(V_x)\, p_x(t, V_w) + g_{x0})\,(V_x - E_x) - g_{TC}\, V_w + g_{TC}\, V_x = 0,$$

that can be solved as in (iii) above.

(v) Solutions for V_x then gave values of $i_x(t)$, the predicted charge movement. These were filed as RK05 arrays possessing a sample interval comparable to those used experimentally, and the same algorithm to determine charge (Huang, 1982) was used for experimental and model arrays.

RESULTS

The experiments used a variety of pulse procedures, but in all of them initial and final steady-state voltages were the same even though the pulse patterns applied to the voltage-clamped fibres varied. In determining charge, all the transients were integrated beyond the point where the final steady current in the 'off' transient was reached. The above approach therefore satisfies the testing condition derived in the Appendix. Two questions were considered: (i) whether the usual criterion of 'on' and 'off' equality suggested on earlier occasions is sufficient to distinguish between resistive and capacitative models, and (ii) whether more complicated pulse procedures can make a clear distinction between these two possibilities. Experimental results from each procedure were in turn compared with predictions from each possible model, but attention was confined to the over-all conservation of charge condition rather than to kinetic details or quantitative discrepancies. In particular, the following differences between the resistive model and experimental results are not considered further. (1) At voltages between −90 and −180 mV the resistive model predicted that there is no non-linear component in the steady-state charge. This is at variance with the experimental findings showing a significant, 15% fall in capacitance per 100 mV hyperpolarization from −90 mV (Huang, 1981*b*). (2) The dependence of capacitance upon depolarizing voltage predicted by the resistive model did not give the inflexions at particular voltages reported experimentally (Huang, 1981*a*, 1982). (3) The resistive model was not consistent with the complex kinetics of the non-linear charge at certain voltages (Adrian & Peres, 1979). However, it is possible that adding further parameters to this model may cover these possibilities.

The approach described in the Methods successfully reproduced the kinetic and steady-state findings illustrated by Matthias *et al.* (1980). The voltage dependence of predicted non-linear charge to large voltage steps from −90 mV was obtained by comparing the transients from a step to test voltage V_T, with those obtained from the voltage-scaled 10 mV reference steps at the holding potential (Adrian & Almers, 1976), and results were in agreement with predictions obtained from the 'equal and opposite' pulse procedure. The results confirm that the resistive model reproduces the approximate 'on' and 'off' equality for large pulses over a wide range of voltages, as required by the experimental findings (Adrian & Almers, 1976). The model could also predict an extra charge moved to a 10 mV step at test voltage V_T as obtained by the pulse procedure of Adrian & Peres (1979). However, as predicted in the Introduction, the equality of 'on' and 'off' charge for the resistive model did not hold for all pulse procedures, and broke down under the following circumstances.

(*1*) *Application of short pulses.* If the imposed voltage step is sufficiently short, so that it ends before full relaxation of the 'on' transient, then a resistive model predicts deviation from 'on' and 'off' charge equality. Thus, the observed conservation of the charge movement to short pulses has been considered to imply an underlying capacitative mechanism (Armstrong & Bezanilla, 1973; Schneider & Chandler, 1973). However, those pulses in which the resistive model did predict deviation from charge conservation had very short durations at which experimental testing was difficult or not possible. Thus Fig. 1 shows the ratio between 'on' and 'off' areas under the transient when the pulse length was progressively shortened from the usual 105 msec for large voltage steps (*A*), in the case illustrated from −90 to −45 mV, at which the experimental non-linearity in the capacitance was large, and for small voltage steps (*B*) from −45 mV to −35 mV. Although it was not possible to obtain the value of $I(\infty)$ at the short pulse lengths, this could be evaluated by introducing bracketting voltage steps using long pulses from which $I(\infty)$ could be obtained for modelled or for experimental results. Although the theoretical 'on'/'off' ratio was relatively independent of voltage and close to 1·0 at most pulse lengths, it fell markedly below 1·0 at short pulse lengths, whereas the experimental transients (Fig. 2) did not show such a trend. However, at such pulse lengths, even with signal averaging of 5–10 sweeps/average, and close sampling frequencies of 200 μsec, the uncertainty in the data became large. This was especially the case for the smaller signals that would be obtained in finding the 'on'/'off' ratio for a small voltage step.

(*2*) *Small voltage steps.* Unlike the case of large voltage steps, the conservation of charge resulting from small voltage steps, as in the procedure of Adrian & Peres (1979), has yet to be tested experimentally. For a capacitative model, provided the transient is allowed to relax fully from the 'off' part of the step, conservation of charge should occur. However, for the resistive model, since (i) the starting values of $R_x(V_T, \infty)$ would now be affected by the prepulse voltage at which the small step was

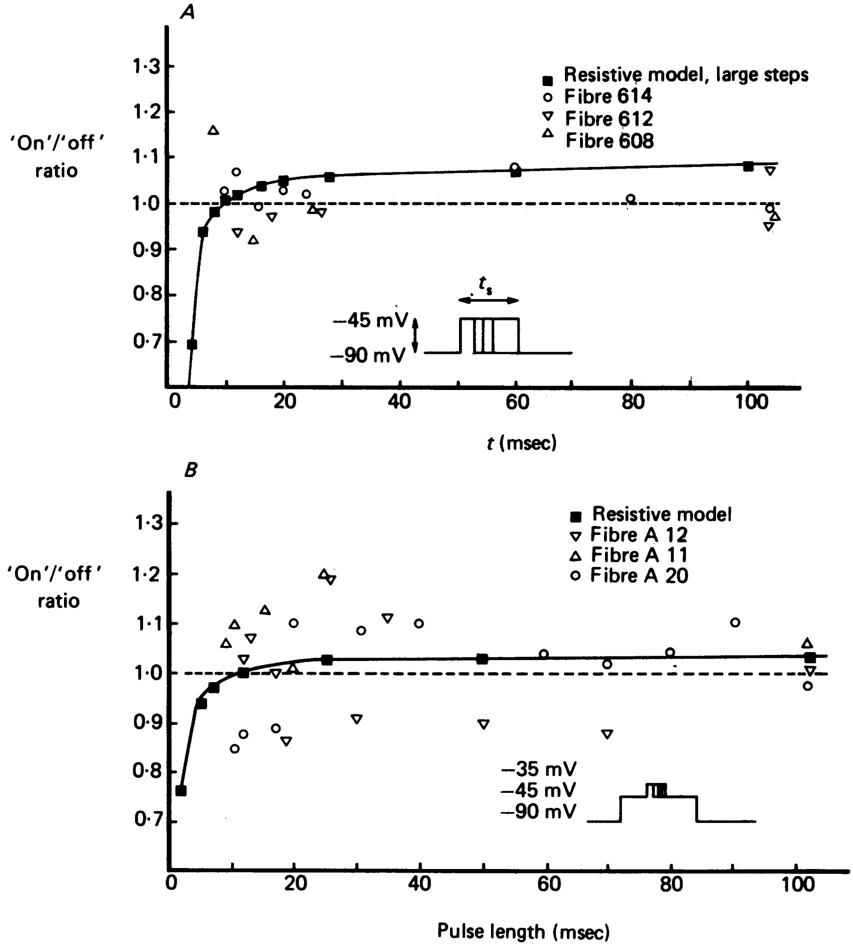

Fig. 1. The ratio of 'on' to 'off' extra charge at different pulse lengths, obtained from: *A*, large 'equal and opposite' voltage steps of ±45 mV from the −90 mV holding potential, or *B*, small steps between −45 and −35 mV, employing a 10 mV step at −90 mV as control. The resistive model (continuous line, ■) predicts marked deviation from a ratio of 1·0 at short (< 15 msec) pulse lengths in both cases, whereas the ratio should remain close to 1·0 for a capacitative model (dashed lines). The scatter of actual experimental data (open symbols) suggests that this usual method of excluding ionic-current type mechanisms is inadequate. Cable constants: *A*: $R_i = 342\ \Omega.\text{cm}$; $\lambda = 3{\cdot}4 \pm 0{\cdot}83$ mm; $r_i = 7047 \pm 310\ \text{k}\Omega/\text{cm}$; diam. $= 112 \pm 34\ \mu\text{m}$; $r_m = 1231 \pm 606\ \text{k}\Omega.\text{cm}$; $R_m = 62{\cdot}6 \pm 41{\cdot}8\ \text{k}\Omega.\text{cm}^2$, $C_m = 12{\cdot}5 \pm 3{\cdot}2\ \mu\text{F/cm}^2$ (three fibres). *B*: $R_i = 322\ \Omega.\text{cm}$, $\lambda = 2{\cdot}75 \pm 0{\cdot}06$ mm, $r_i = 7032 \pm 802\ \text{k}\Omega/\text{cm}$; diam. $= 77{\cdot}3 \pm 3{\cdot}61\ \mu\text{m}$; $r_m = 550 \pm 72{\cdot}2\ \text{k}\Omega.\text{cm}$; $R_m = 12{\cdot}99 \pm 1{\cdot}125\ \text{k}\Omega.\text{cm}^2$; $C_m = 7{\cdot}7 \pm 1{\cdot}32\ \mu\text{F/cm}^2$ (three fibres).

being taken, and (ii) the 'off' transient current would now be subject to a varying 'off' voltage, which would affect both the (voltage-dependent) kinetic parameters of, and driving force of the current through, R_x, this equality need not be the case. Thus the numerical solutions predicted that the 'on' non-linear charge could be up to 20 % greater than the 'off' charge, as it was at voltages between −80 and −40 mV, near the foot of the non-linear dependence of the charge upon the voltage. This was in

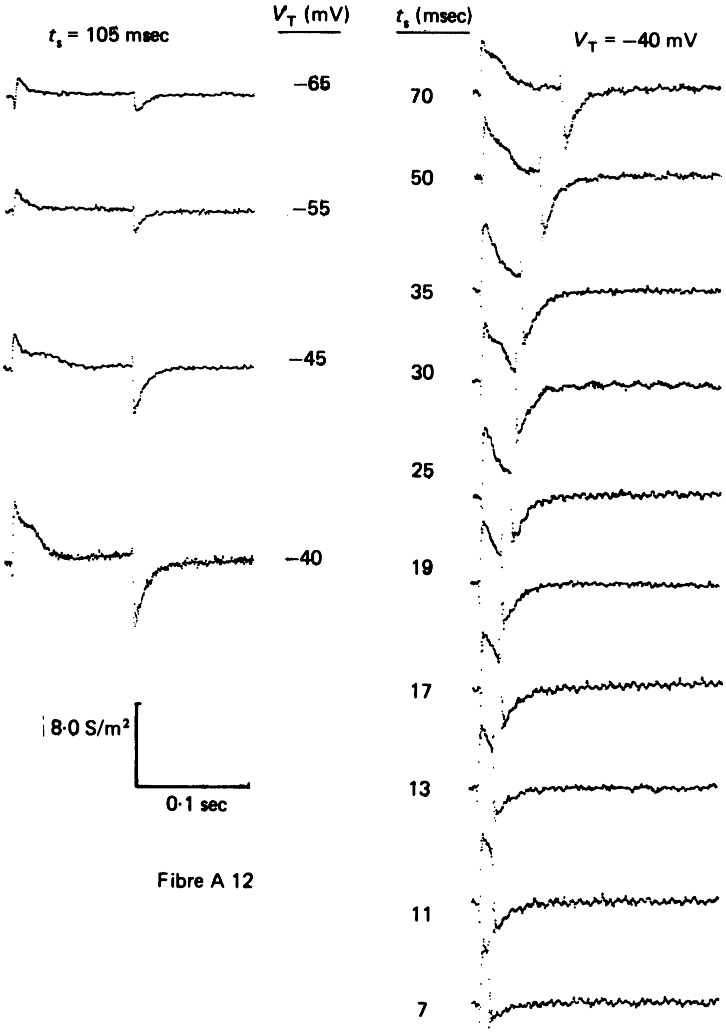

Fig. 2. Left: Employing long pulses established that imposing a voltage step between −45 and −35 mV examines both q_β and q_γ components of non-linear charge. Right: charge movements in response to voltage steps between −45 and −35 mV of varying lengths. In estimating the steady-state current $I(\infty)$, transients from a long pulse were used. The integrated transients were approximately equal for 'on' and 'off' pulses even at the shortest pulse lengths. Fibre in hypertonic solution; temperature 5·2 °C. $R_i = 322\ \Omega\,.\,\text{cm}$; $\lambda = 2{\cdot}82$ mm; $r_i = 8820\ \text{k}\Omega/\text{cm}$; diam. = 70 μm; $r_m = 704\ \text{k}\Omega\,.\,\text{cm}$; $R_m = 15{\cdot}1\ \text{k}\Omega\,.\,\text{cm}^2$; $C_m = 7{\cdot}4\ \mu\text{F}/\text{cm}^2$.

contrast to the values from experimental results (Table 1); these were more consistent with a capacitative model predicting a voltage-independent ratio of 1·0. Thus the variance of the data about the predictions of a resistive model was 50 % greater than had a capacitative model been assumed.

(3) *Application of a superimposed hyperpolarization.* More striking distinctions between the results expected from capacitative and resistive models of charge movements required introduction of more complex pulse procedures. The following

TABLE 1. Experimental and predicted values of the ratio of 'on' to 'off' non-linear charge at different voltages (seven fibres)

		Predicted	
Voltage	Experimental	Resistive model	Capacitative model
−65	1·049 ± 0·130	1·253	1·0
−55	0·935 ± 0·031	1·132	1·0
−50	0·885 ± 0·007	1·070	1·0
−45	0·866 ± 0·052	1·045	1·0
−40	1·067 ± 0·020	1·015	1·0
−35	1·011 ± 0·014	1·012	1·0
−25	0·938 ± 0·041	0·999	1·0

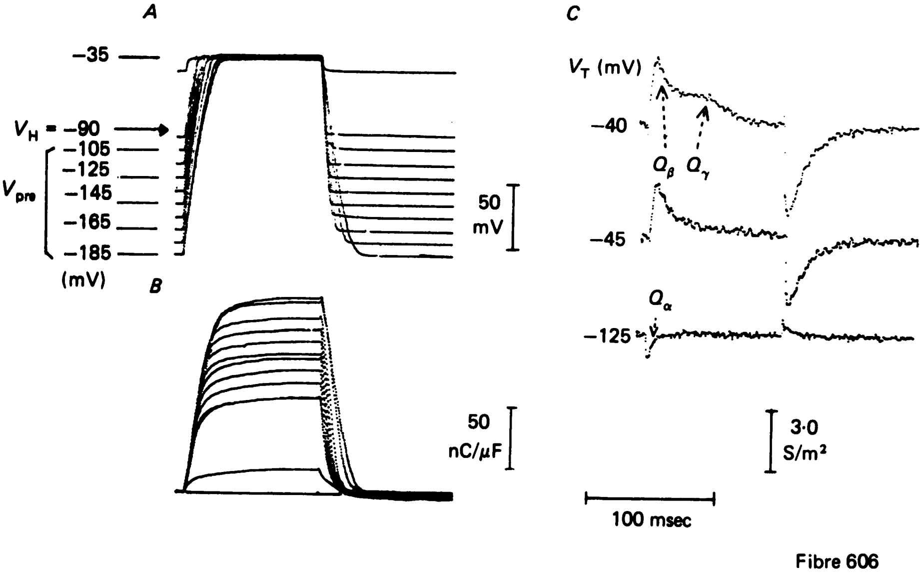

Fig. 3. Effect of voltage-clamp steps to −35 mV from varying prepulse potentials, V_{pre}. *A*, voltage traces of the actual clamp steps taken. Although the voltage-clamp steps were not perfectly rectangular, the steady voltages to which the steps tended was the same, and the size of the step could be measured directly from the traces. *B*, the running integral of the transient current, obtained on-line, implies zero net charge moved at the end of all the steps. *C*, investigating the extra charging current to small steps in the same fibres at different voltages demonstrated that this procedure includes sufficient voltage range to examine all three reported components (q_α, q_β and q_γ) of non-linear charge (Huang, 1982). Temperature 3·1 °C; $R_i = 344\ \Omega.\text{cm}$; $\lambda = 3{\cdot}2$ mm; $r_i = 7074\ \text{k}\Omega/\text{cm}$; diam. = 79 μm; $r_m = 722\ \text{k}\Omega.\text{cm}$; $R_m = 17{\cdot}9\ \text{k}\Omega.\text{cm}^2$; $C_m = 10{\cdot}8\ \mu\text{F}/\text{cm}^2$. Four sweeps/average.

pulse programme, shown in Fig. 4 (inset), exploited the voltage dependence of the driving force on the non-linear current expected had this an ionic basis. (i) The membrane was stepped from a −90 mV holding potential to a series of prepulse voltages for 500 msec, which was of ample duration to allow full relaxation of the transient. Where the prepulse voltage was hyperpolarized to the holding potential, this transient should consist exclusively of linear charge, since the non-linear R_x was inactive at such voltages. (ii) The prepulse was then followed by the 'on' voltage step to a fixed membrane potential of −35 mV. Its duration of 105 msec was also sufficient to allow full relaxation of both linear and non-linear parts of the transient. (iii) The clamped potential was next stepped back to the prepulse voltage for 105 msec in the 'off' step, before returning to the holding potential of −90 mV. Five such sweeps were recorded for averaging into each experimental trace. (iv) The amount of 'non-linear' transient charge that had moved through the 'on' and 'off' steps respectively were determined for both experimental and predicted traces from the resistive model. This procedure employed a linear, reference charge corresponding to the integral of the transient resulting from a 10 mV step at −180 mV. In finding the amount of non-linear charge, this value was scaled to the actual potential excursions entailed by the applied voltage steps. The reference voltage was thus consistent and independent of any residual non-linear capacitance that might exist in the experimental traces between −90 and −180 mV. The voltage steps could be computed directly from actual and experimental voltage traces (Fig. 3*A*) obtained by multiplexing sampling of the current and voltage channels. As the voltage perturbations were not perfect steps, and involved large potential excursions, the leak admittance correction applied was obtained from the voltage trace $V(t)$ scaled by $I(\infty)/V(\infty)$.

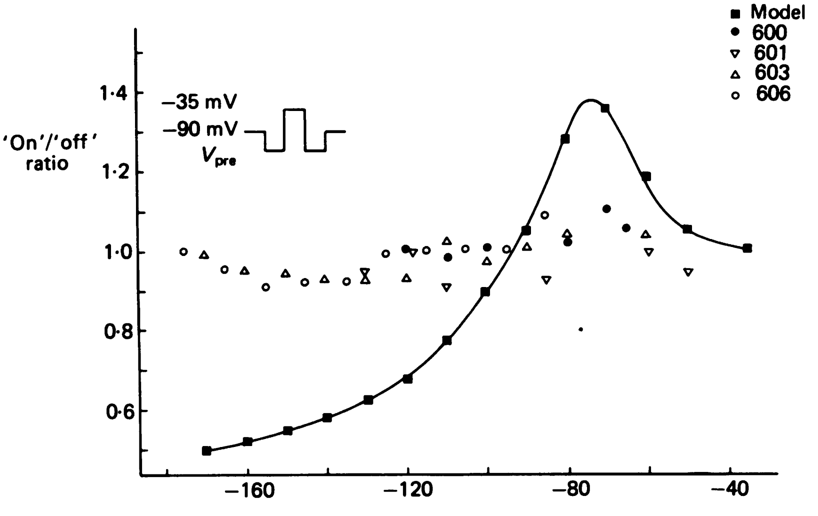

Fig. 4. Dependence of the ratio between 'on' and 'off' non-linear charge (ordinate) upon the pre- and post-pulse potential, V_{pre} (abscissa) superimposed upon a voltage step to −35 mV. The resistive model (continuous line, ■) predicts a marked dependence of this ratio upon the voltage. This is not reflected in the experimental ratios (remaining symbols), whose values are relatively independent of voltage and close to 1·0. Four fibres. $R_i = 342\ \Omega.\text{cm}$; $\lambda = 2{\cdot}42 \pm 0{\cdot}27$ mm; $r_i = 7367 \pm 520\ \text{k}\Omega/\text{cm}$; diam. $= 76 \pm 7{\cdot}6\ \mu\text{m}$; $r_m = 466 \pm 91\ \text{k}\Omega.\text{cm}$; $R_m = 10{\cdot}9 \pm 2{\cdot}24\ \text{k}\Omega.\text{cm}^2$; $C_m = 9{\cdot}5 \pm 1{\cdot}27\ \mu\text{F/cm}^2$.

In the above procedure, the initial and final steady values of the applied potential were identical. Hence, a capacitative model would predict equal 'on' and 'off' integrals of the non-linear part of the transient current. However, this was not the prediction from the resistive model since the postulated non-linear charge carrier is an ionic current. The absolute driving force for the 'off' current across R_x is then a function of the difference between the post-pulse voltage and its effective postulated reversal potential, E_x of -90 mV. Hence, although the kinetic parameters for R_x possessed a dependence upon voltage causing an asymmetrical time course of R_x that resulted in equality of charge when voltage steps were applied from one particular potential, this need not be the case at other potentials. For example, a returning 'off' step to a potential hyperpolarized to E_x would increase the net driving force of current through the series resistance, and increase the 'returning' current even when the 'on' transient was being determined largely by the test voltage at -35 mV. This would result in an 'off' being greater than the 'on' non-linear charge at hyperpolarized prepulses. The converse could apply if the prepulses were at potentials depolarized to E_x, even when the absolute potential of the 'on' step was kept constant.

These expectations for the resistive model were confirmed by numerical solution. The predictions were at variance with the experimental results which were consistent with a voltage-independent 'on'/'off' ratio for non-linear charge close to 1·0. Thus Fig. 3 shows: *A*, traces of the clamp voltage, V_1, in a muscle fibre employing steps to a fixed voltage of -35 mV from successively hyperpolarized prepulses, and *B*, running integrals $\int \mathrm{d}Q$ of the transient part of the total current computed on-line, demonstrating zero net charge at the end of the off step. This is in contrast to the predicted 'on'/'off' ratio of non-linear charge (Fig. 4) for the resistive model, for which the numerical solutions implied the following. (i) The 'on'/'off' ratio is heavily dependent upon voltage; (ii) the only prepulse voltages at which the 'on'/'off' ratio is close to 1 are where the pulses are taken from potentials close to between -90 and -100 mV, which however, corresponds to the same condition under which the parameters of the model were derived, and the limiting case where the prepulse approximates the test voltage; (iii) at voltages hyperpolarized to around -90 mV, the area under the 'off' transient is appreciably greater than that under the 'on' transient. This is a large effect; the 'on'/'off' ratio fell to below 0·5 at large hyperpolarizations close to -180 mV; (iv) at voltages between -90 mV and the test voltage, the 'on' charge exceeded the 'off', and the 'on'/'off' ratio rose to around 1·3 at prepulse potentials of -70 mV. The predictions of the resistive model were thus at variance with the experimental data, whose ratios of 'on' to 'off' non-linear charge remained close to 1·0, and were not significantly dependent upon prepulse potential. Thus they gave a regression line of slope $0{\cdot}00107 \pm 0{\cdot}00004$/mV. Furthermore, the variance of the experimental points about the possible predictions was 17 times greater by assuming the resistive, as compared to the capacitative, model.

(4) 'Staircase' pulse sequences. The previous pulse procedure was essentially a test for the conservation of charge conditions through a series of transients beginning and ending in a given steady-state voltage. On the same principle, it should be possible to design a pulse cycle incorporating a series of steady states but ending at the initial voltage. To this end, the following simple pulse cycle was considered.

(A) For the resistive model (i) the transient part of the non-linear current was integrated for a large 'on' voltage step from the -90 mV holding potential to a test voltage of -40 (or -30) mV to give a 'forward' non-linear charge; (ii) the voltage interval between -90 and -40 mV was divided into a series of 10 mV 'off' steps, through which the fibre was returned to the holding potential of -90 mV. Each small step was of sufficient duration (105 msec) to allow full relaxation of the current transient in each stage; (iii) the area under the transient for each 'off' step was measured and given a negative sign (since it was a 'return' charge) and used in plotting the net steady non-linear charge moved through the pulse cycle. Fig. 5 displays the charge predicted from the resistive model in response to large steps (dotted lines), and the non-linear steady charge as the voltage returns in a 'staircase' of 10 mV stages to the initial potential of -90 mV from -30 mV or -40 mV. A form of 'hysteresis' appears to occur in the charge–voltage relationship in that the net charge moved on the returning limb of the curve (continuous lines) does not superimpose upon the dependence of non-linear charge on potential when employing large voltage steps; this is so even though the reference charge from which the total charge is subtracted was the same 10 mV step from -100 mV in both cases. Such a prediction of a net charge not being a single-valued function of potential is not consistent with a capacitative model (see Appendix). Furthermore, Fig. 5 also shows that moving the resistive model through a pulse cycle even of this simple type results in a net movement of 4·5 nC/μF of non-linear charge on returning to the initial value of the potential, out of the forward 14·3 nC/μF resulting charge from the forward step to -40 mV. Effects of this kind were most clearly demonstrable at the foot of

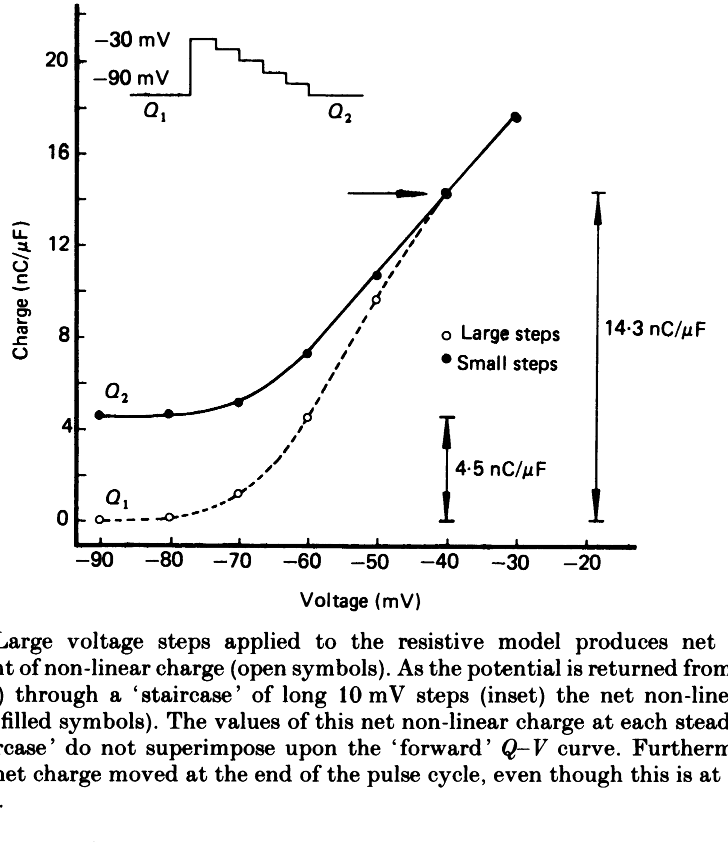

Fig. 5. Large voltage steps applied to the resistive model produces net 'forward' movement of non-linear charge (open symbols). As the potential is returned from -40 mV (arrowed) through a 'staircase' of long 10 mV steps (inset) the net non-linear charge declines (filled symbols). The values of this net non-linear charge at each steady state in the 'staircase' do not superimpose upon the 'forward' Q–V curve. Furthermore there remains net charge moved at the end of the pulse cycle, even though this is at the initial potential.

the Q–V relationship, where 30% or more of the non-linear charge did not return when the voltage was re-set in a series of steps. Plots of this type showed in large voltage steps to -30, -40, -50, -60 and -70 mV that 26, 32, 35, 39 and 61% respectively of the non-linear charge moved forwards would not return on repolarizing the fibre back to -90 mV holding potential in small 10 mV steps. These rather complex predictions differ from the capacitative case, where the net charge measured at the end of the pulse cycle should be zero whatever the path.

(B) The two contrasting predictions were tested experimentally as follows: (i) The voltage-clamped muscle fibre was subjected to a single large depolarizing voltage step from its -90 mV holding potential; five such identical sweeps were taken for averaging into each record. Comparing the transient current so obtained with that resulting from a control 10 mV step at -100 mV appropriately scaled by the ratio of the size of the test and control voltage perturbations, gave the non-linear current to the large test-voltage step. The total non-linear charge moved could then be obtained through numerical integration. Fig. 6*A* shows one such running integration of the 'on' part of this non-linear transient in response to a voltage step from -90 to -40 mV. The two components *a* and *b* in the rising part of the integration imply the step was sufficiently large to involve both q_β and q_γ components respectively in the response. However, the trace plateaus to a steady value (in this case, 11·5 nC/μF). These values are plotted for the several individual fibres studied and are shown as the points arrowed in Fig. 7. (ii) The same fibre was then subjected to a series of 10 mV steps at varying voltages. Both 'on' and 'off' parts were of sufficient duration (105 msec) to allow the resulting transients to relax fully. The voltages from which these small steps were taken were in 10 mV increments spanning the values of the holding potential and the voltage resulting from the initial large step. (iii) The non-linear part of the 'off' transients were integrated to give the charge returning to each 'off' step. Fig. 6*B* shows a series of the corresponding running integrals as a progression *c*–*g*, of decrements in net charge from that resulting from the initial forward step. This demonstrated that the non-linear charge progressively returned

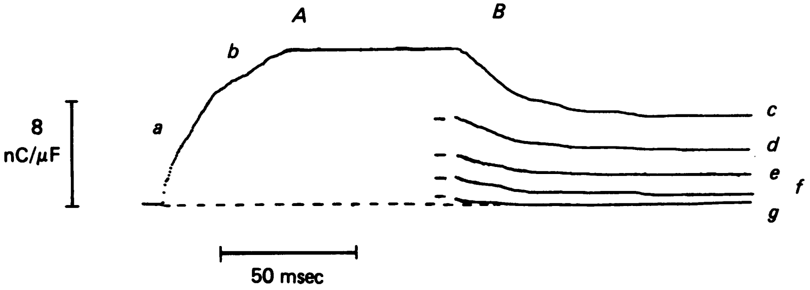

Fig. 6. *A*, running integral of the transient part of the non-linear current obtained from a large voltage step from -90 to -40 mV. The trace rises in two stages (*a* and *b*) to a steady final value. *B*, successive running integrals reconstructing progressive declines (*c*–*g*) in net charge as the potential is returned through a 'staircase' of 10 mV steps to its initial value. There is close to zero net charge at the end of the pulse cycle. Fibre cable constants: $R_i = 341\ \Omega.\text{cm}$; $\lambda = 3{\cdot}5$ mm; $r_i = 5269\ \text{k}\Omega/\text{cm}$; diam. = 91 μm; $r_m = 647\ \text{k}\Omega.\text{cm}$; $R_m = 18{\cdot}4\ \text{k}\Omega.\text{cm}^2$; $C_m = 9{\cdot}7\ \mu\text{F}/\text{cm}^2$.

through the potential 'staircase' with a net non-linear charge moved close to zero. (iv) The net charge at successive steps in the pulse series could therefore be plotted (Fig. 7, points on continuous line) through the successive steady-state voltages. Such a plot showed from several fibres that this procedure would result in no significant net charge moved through this pulse cycle. Thus the value of this charge was $0{\cdot}1 \pm 0{\cdot}46$ nC/μF (S.E. of the mean), a value not significantly different ($P \gg 5\%$) on *t*-testing from the null hypothesis of zero net charge. This is consistent with the conservation prediction of the capacitative model and not the resistive model.

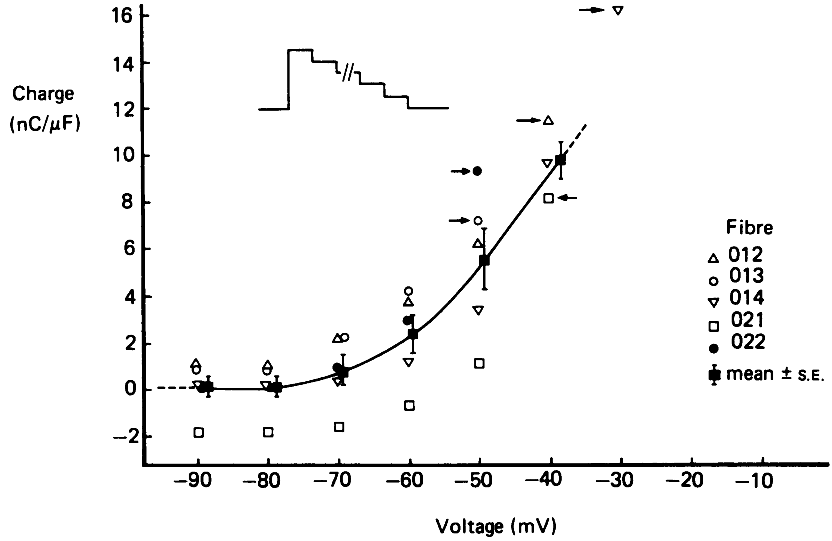

Fig. 7. The 'staircase' pulse procedure reconstructed for experimental muscle fibres. 'On' non-linear charge (arrowed points) was computed for large voltage steps from −90 mV. The net charge through a succession of steady states produced by the 'staircase' of small 10 mV return steps to the holding potential is plotted as data points and their mean ± S.E. of the mean. On returning to the initial voltage, there is no significant net charge moved as a result of the pulse cycle. This contradicts predictions of the resistive model. Five fibres. $R_i = 342\ \Omega.\mathrm{cm}$; $\lambda = 3{\cdot}02 \pm 0{\cdot}1$ mm; $r_i = 3485 \pm 432\ \mathrm{k\Omega/cm}$; diam. $= 114{\cdot}5 \pm 6{\cdot}1\ \mu$m; $r_m = 338 \pm 80\ \mathrm{k\Omega.cm}$; $R_m = 11{\cdot}66 \pm 2{\cdot}31\ \mathrm{k\Omega.cm^2}$; $C_m = 13{\cdot}1 \pm 1{\cdot}1\ \mu\mathrm{F/cm^2}$.

DISCUSSION

The experiments described were explicitly directed at assessing the nature of the transient part of the non-linear current in response to voltage steps, referred to as charge movement. They employed a wider range of pulse criteria than in earlier work, in which the major argument for invoking a capacitative mechanism was the equality of 'on' and 'off' non-linear charge elicited by large voltage steps. This further investigation was prompted by the models of Matthias *et al.* (1980) which employed a *linear* capacitative element, yet in which some of the major equilibrium and transient experimental findings of the non-linear charge were successfully reproduced through suitable non-linearities in the resistive elements. In particular, the model mimicked the 'on' and 'off' equality of the charge transient obtained from large imposed voltage steps. This paper confirms this finding. It goes on, however, to show that the charge conservation so produced is not a general one. For example, shortening the 'on' pulse durations did cause the equality to break down. Nevertheless, this was at pulse durations that made experimental assessment difficult, and so the resistive model of the charge movement is of value in pointing out that merely a single instance of charge conservation is inadequate to establish the mechanism underlying the observed currents. Thus it was shown that the resistive model remains fully consistent with earlier data concerning the conservation of charge.

Designing a wider series of tests used as its basis the analysis of Duane & Huang (1982) that expressed the steady-state charge uniquely in terms of its state variables of voltage and temperature, independently of the detailed dynamics of the underlying system. From this the Appendix derived the over-all properties of the charge analytically in a general form: (i) the steady-state charge is a function of voltage; (ii) the charge saturates, and (iii) charge is *conserved* through all paths $\mathbf{r}$ taken by the state variables as a function of time. The issue at hand concerns the physical interpretation of the integral of the transient current in response to a voltage step. Hence testing condition (iii) involved the use of voltage steps, and within such constraints the following pulse procedures were devised: (*a*) small steps of constant size but from varying voltages, (*b*) superimposed hyperpolarization on voltage steps to a constant test potential, and (*c*) pulse cycles involving several successive steady-state voltages. All these protocols were made to satisfy the condition of common initial and final state variables. Hence conditions (i)–(iii) above would predict zero net charge moved ('on' and 'off' equality) at the end of each procedure, for a capacitative charge. This was indeed the case experimentally and the findings therefore remain fully consistent with a capacitative description of the charge movement.

Such a generalized conservation condition, however, need not apply in the resistive model. Admittedly, it was not possible to derive steady-state features or any generalizations of the above kind analytically for models of this kind. This reflects the complicated non-linearities involved in the resistive elements in producing both dependence of charge upon voltage, and conservation of charge in the single type of pulse procedure considered. Nevertheless, numerical solutions for such a circuit showed that conservation of charge broke down in all the additional conditions tested except where they corresponded to procedures precisely identical to those under which the alternative model was originally constructed. Elsewhere, 'on'/'off' ratios markedly deviated from 1·0 and became noticeably dependent upon potential. In addition to these qualitative differences, one could go further to point out that resistive models still do not consider complexities in the kinetics of the charge movement, nor persistent non-linearities observed at hyperpolarized voltages. It is conceivable that adding further parameters may generate altered predictions consistent with all these findings. However, as it stands, the resistive model is already substantially complex. For example the non-linearity in R_x only produces the rather limited conservation of charge discussed, and more complicated versions of the resistive model invoke rectification in other resistive elements to result in an over-all voltage dependence in $I(\infty)$ that saturates the non-linear charge at extreme potentials. This entails additionally introducing complicated rectifications also in two other resistive circuit elements. In contrast, the capacitative description derives all these findings from a single equation analytically and independent of kinetics. It would appear reasonable, therefore, to justify further models of the resistive type first through the demonstration of specific experimental instances in which the capacitative description breaks down, employing a necessary condition of which the one employed in this paper is a simple example.

APPENDIX

Duane & Huang (1982) introduced a statistical mechanical description of the steady-state properties of a non-linear capacitance, independent of its dynamics beyond the assumption that transitions between the energy states, j, of microscopic energies ϵ_j, available to the system can occur, in order that equilibrium can be achieved. They thus derived an analytic single-valued expression for the macroscopic steady-state non-linear charge movement, $\int \mathrm{d}Q$, in a manner independent of any non-equilibrium features, including non-linearities in the rate constants describing transitions between permitted states and details of the transient responses in the subsystems. From their analysis, this Appendix derives a general statement concerning saturation and conservation of the non-linear charge in terms of its state variables of voltage and temperature. The formalisms from that paper that will be employed are as follows.

(i) The partition function of the system is:

$$Z = \sum_j \mathrm{e}^{-\epsilon_j(V)/kT}, \tag{1}$$

where k is the Boltzmann constant, T the absolute temperature; the dependence of the microsopic energy of each state available to the subsystem involved, $\epsilon_j(V)$ can be written as a smooth power series in voltage V.

(ii) Each element (subsystem) in the systems examined contributes a microscopic steady-state charge movement given by

$$\langle q\rangle = \frac{kT}{Z}\cdot\frac{\partial Z}{\partial V}. \tag{2}$$

(iii) The macroscopic charge movement for the ensemble of subsystems assuming number density L, is

$$\int \mathrm{d}Q = \int_{V_0}^{V} LkT\left(\frac{1}{Z}\frac{\partial^2 Z}{\partial V^2} - \left(\frac{1}{Z}\cdot\frac{\partial Z}{\partial V}\right)^2\right)\mathrm{d}V, \tag{3}$$

where V_0 is a reference or control voltage.

(1) Saturation of charge implies zero partial derivative of the macroscopic charge $\int \mathrm{d}Q$ with respect to voltage at large absolute values of the applied voltage, $|V|$. Equation (2) gives

$$\langle q\rangle = \frac{kT}{Z}\cdot\frac{\partial Z}{\partial V}; \quad \text{hence} \quad \langle q^2\rangle = \frac{(kT)^2}{Z}\cdot\frac{\partial^2 Z}{\partial V^2} \qquad \text{from eqn. (1)}$$

and so, from eqn. (3),

$$\left(\frac{\partial Q}{\partial V}\right)_T = L[\langle q^2\rangle - \langle q\rangle^2]/kT.$$

For large positive *or* negative voltages, V, the partition function Z is dominated by that term with the largest $q_j V$, say q_N. Hence the expectancy P_N for state N tends to 1·0, and the other expectancies, P_j, $j \neq N$, vanish. This gives

$$\langle q \rangle = \sum_j q_j P_j \rightarrow q_N$$

$$\langle q^2 \rangle = \sum_j q_j^2 P_j \rightarrow q_N^2,$$

so $\langle q^2 \rangle - \langle q \rangle^2$ tends to zero, or,

$$\lim_{|V| \to \infty} \left(\frac{\partial Q}{\partial V}\right)_T = \frac{L}{kT} \lim_{|V| \to \infty} [\langle q^2 \rangle - \langle q \rangle^2] = 0,$$

and the charge saturates at large absolute values of the voltage.

(2) The conservation of charge condition can be made to apply for *any* path R in the voltage–temperature (V, T) plane from an initial steady state S to a final steady state S'. If R is represented parametrically in time on the vector,

$$\mathbf{r}(t) = \mathbf{i}\,V(t) + \mathbf{j}T(t),$$

then S corresponds to $t = -\infty$, S' to $t' = +\infty$, and $(\mathbf{i}, \mathbf{j})$ are the unit vectors for voltage and temperature expressed as functions of time. $V(t)$, $T(t)$ respectively. From eqn. (3), it can be seen that the total differential coefficient $\mathrm{d}Q$ in any domain D in the (V, T) plane is the line integral

$$\int_S^{S'} \mathrm{d}Q = \int_S^{S'} \left[\left(\frac{\partial Q}{\partial V}\right)_T \frac{\mathrm{d}V}{\mathrm{d}t} + \left(\frac{\partial Q}{\partial T}\right)_V \cdot \frac{\mathrm{d}T}{\mathrm{d}t}\right] \mathrm{d}t.$$

The identity,

$$\lim_{\delta t \to 0} \delta Q = \left(\frac{\partial Q}{\partial V}\right)_T \delta V + \left(\frac{\partial Q}{\partial T}\right)_V \delta T,$$

gives the exact differential

$$\int_S^{S'} \mathrm{d}Q = \int_t^{t'} \frac{\mathrm{d}Q}{\mathrm{d}t} \cdot \mathrm{d}t = Q[V(t), T(t)] \Big|_{t=-\infty}^{t'=\infty}$$

$$= Q(V_1, T_1) - Q(V_0, T_0)$$

where (V_0, T_0), (V_1, T_1) are the co-ordinates for the initial and final steady-state variables. The term $\int_t^{t'} \frac{\mathrm{d}Q}{\mathrm{d}t} \cdot \mathrm{d}t$ is the integral of the current of capacitative origin which to a voltage step is given by $\int (I(t) - I(\infty))\mathrm{d}t$. Hence for this current, the measured charge moved through the path, R, $\int_R \mathrm{d}\mathbf{Q}\, \mathrm{d}\mathbf{r}$, is independent of the path $\mathbf{r}(t)$ of $V(t)$ and $T(t)$.

The above condition implies that for a simple *closed* path R, divided into arcs R', R'' in domain D, the line integral

$$\int_{R'} \mathrm{d}Q = -\int_{R''} \mathrm{d}Q, \quad \text{or} \quad \int_{R'} \mathrm{d}Q \Big/ \left(-\int_{R''} \mathrm{d}Q\right) = 1.$$

This includes the condition for 'on' and 'off' equality to a voltage step used in the experiments described above. An alternative statement of this condition is that for every simple closed path R in D, the contour integral of the net charge,

$$\oint \mathrm{d}Q = 0$$

and the field of force given by $\mathrm{d}Q$ is *conservative*. This is the condition used in the last experiment described above.

The author thanks Professor R. H. Adrian and Dr S. Duane for helpful discussions, and Professor W. K. Chandler for reading and commenting on the manuscript. Mr W. Smith provided skilled assistance.

REFERENCES

ADRIAN, R. H. & ALMERS, W. (1976). Charge movement in the membrane of striated muscle. *J. Physiol.* **254**, 339–360.

ADRIAN, R. H. & PERES, A. (1979). Charge movement and membrane capacity in frog muscle. *J. Physiol.* **289**, 83–97.

ADRIAN, R. H. & RAKOWSKI, R. F. (1978). Reactivation of membrane charge movement and delayed potassium conductance in skeletal muscle fibres. *J. Physiol.* **278**, 533–557.

ARMSTRONG, C. M. & BEZANILLA, F. (1973). Currents related to movement of the gating particles of the sodium channels. *Nature, Lond.* **242**, 459–461.

BRENT, R. P. (1973). Algorithms for minimizations without derivatives. Englewood Cliffs, NJ: Prentice Hall.

CHANDLER, W. K., RAKOWSKI, R. F. & SCHNEIDER, M. F. (1976). A non-linear voltage-dependent charge movement in frog skeletal muscle. *J. Physiol.* **254**, 245–283.

DUANE, S. & HUANG, C. L.-H. (1982). A quantitative description of the voltage-dependent capacitance in frog skeletal muscle in terms of equilibrium statistical mechanics. *Proc. R. Soc.* B **215**, 75–94.

GILLY, W. F. (1981). Intramembrane charge movements and excitation–contraction coupling. In *The Regulation of Muscle Contraction. Excitation–Contraction Coupling*, ed. GRINNELL, A. D. & BRAZIER, MARY A. B., pp. 3–22. New York: Academic Press.

HODGKIN, A. L. & NAKAJIMA, S. (1972). The effect of diameter on the electrical constants of frog skeletal muscle fibres. *J. Physiol.* **221**, 105–120.

HOROWICZ, P. & SCHNEIDER, M. F. (1981). Membrane charge moved at contractile thresholds in skeletal muscle fibres. *J. Physiol.* **314**, 595–633.

HUANG, C. L.-H. (1981*a*). Dielectric components of charge movements in skeletal muscle. *J. Physiol.* **313**, 187–205.

HUANG, C. L.-H. (1981*b*). Membrane capacitance in hyperpolarized muscle fibres. *J. Physiol.* **313**, 207–222.

HUANG, C. L.-H. (1982). Pharmacological separation of charge movement components in frog skeletal muscle. *J. Physiol.* **324**, 375–387.

MATTHIAS, R. T., LEVIS, R. A. & EISENBERG, R. S. (1980). Electrical models of excitation–contraction coupling and charge movement in skeletal muscle. *J. gen. Physiol.* **76**, 1–31.

MATTHIAS, R. T., LEVIS, R. A. & EISENBERG, R. S. (1981). An alternative interpretation of charge movement in muscle. In *The Regulation of Muscle Contraction. Excitation–Contraction Coupling*, ed. GRINNELL, A. D. & BRAZIER, MARY A. B., pp. 39–54. New York: Academic Press.

SCHNEIDER, M. F. & CHANDLER, W. K. (1973). Voltage-dependent charge movement in skeletal muscle: a possible step in excitation–contraction coupling. *Nature, Lond.* **242**, 244–246.